

# Measurement of high order Kerr refractive index of major air components

V. Loriot, E. Hertz, O. Faucher, and B. Lavorel

Institut Carnot de Bourgogne, UMR 5209 CNRS-Université de Bourgogne  
BP 47870, 21078 Dijon Cedex, France

[Bruno.Lavorel@u-bourgogne.fr](mailto:Bruno.Lavorel@u-bourgogne.fr)

**Abstract:** We measure the instantaneous electronic nonlinear refractive index of  $N_2$ ,  $O_2$ , and Ar at room temperature for a 90 fs and 800 nm laser pulse. Measurements are calibrated by post-pulse molecular alignment through a polarization technique. At low intensity, quadratic coefficients  $n_2$  are determined. At higher intensities, a strong negative contribution with a higher nonlinearity appears, which leads to an overall negative nonlinear Kerr refractive index in air above 26 TW/cm<sup>2</sup>.

© 2009 Optical Society of America

**OCIS codes:** (320.2250) Femtosecond phenomena; (350.5400) Plasmas; (190.7110) Ultrafast nonlinear optics; (260.5950) Self-focusing

---

## References and links

1. A. Couairon and A. Mysyrowicz, "Femtosecond filamentation in transparent media," *Phys. Rep.* **441**, 47-189 (2007).
2. E. T. J. Nibbering, G. Grillon, M. A. Franco, B.S. Prade, and A. Mysyrowicz, "Determination of the inertial contribution to the nonlinear refractive index of air  $N_2$ , and  $O_2$  by use of unfocused high-intensity femtosecond laser pulses," *J. Opt. Soc. Am. B* **14**, 650-660 (1997). J-F. Ripoche, G. Grillon, B. Prade, M. Franco, E. Nibbering, R. Lange, and A. Mysyrowicz, "Determination of the time dependence of  $n_2$  in air," *Opt. Comm.* **135**, 310 (1997).
3. A. Couairon, "Dynamics of femtosecond filamentation from saturation of self-focusing laser pulses," *Phys. Rev. A* **68**, 015801 (2003).
4. R. Nuter and L. Bergé, "Pulse chirping and ionization of  $O_2$  molecules for the filamentation of femtosecond laser pulses in air," *J. Opt. Soc. Am. B* **23**, 874-884 (2006).
5. P. Sprangle, E. Esarey, and B. Hafizi, "Propagation and stability of intense laser pulses in partially stripped plasmas," *Phys. Rev. E* **56** 5894-5907 (1997).
6. H. Stapelfeldt and T. Seideman, "Colloquium: Aligning molecules with strong laser pulses," *Rev. Mod. Phys.* **75** (2), 543-557 (2003).
7. V. Renard, M. Renard, S. Guérin, Y. T. Pashayan, B. Lavorel, O. Faucher, and H. R. Jauslin, "Postpulse Molecular Alignment Measured by a Weak Field Polarization Technique," *Phys. Rev. Lett.* **90** (15), 153601 (2003).
8. V. Loriot, P. Tzallas, E. P. Benis, E. Hertz, B. Lavorel, D. Charalambidis and O. Faucher, "Laser-induced field-free alignment of the OCS molecule," *J. Phys. B* **40**, 2503-2510 (2007).
9. Maroulis, "Accurate electric multipole moment, static polarizability and hyperpolarizability derivatives for  $N_2$ ," *J. Chem. Phys.* **118** 2673-2687 (2003).
10. E. Hertz, B. Lavorel, O. Faucher, and R. Chaux, "Femtosecond polarization spectroscopy in molecular gas mixtures: Macroscopic interference and concentration measurements," *J. Chem. Phys.*, **113** 6629-33 (2000).
11. R. W. Boyd, *Nonlinear optics* third ed. Academic Press (2007).
12. V. Loriot, E. Hertz, B. Lavorel and O. Faucher, "Field-free molecular alignment for measuring ionization probability," *J. Phys. B* **41** 015604 (2008).
13. P. Neogrády, M. Medvėd, I. Černušák, and M. Urban, "Benchmark calculations of some molecular properties of  $O_2$ , CN and other selected small radicals using the ROHF-CCSD(T) method," *Mol. Phys.* **100**, 541 (2002)
14. J. Arabat and J. Etchepare, "Nonresonant fifth-order nonlinearities induced by ultrashort intense pulses," *J. Opt. Soc. Am. B* **10**, 2377-82 (1993).
15. V. Loriot, P. Béjot, E. Hertz, O. Faucher, B. Lavorel, S. Henin, J. Kasparian, and J.-P. Wolf, "Higher-order Kerr terms allowing ionization-free filamentation in air," *Submitted to Phys. Rev. Lett.*

16. G. Méchain, A. Couairon, Y.-B. André, C. d'Amico, M. Franco, B. Prade, S. Tzortzakis, A. Mysyrowicz, R. Sauerbrey, "Long-range self-channeling of infrared laser pulses in air: a new propagation regime without ionization," *Appl. Phys. B* **79**, 379 (2004)
- 

## 1. Introduction

The propagation of intense short laser pulses in the atmosphere is an important domain of investigation regarding applications in remote sensing. This propagation is accompanied by a number of phenomena among which one finds self-focusing and self-phase modulation, ionization and plasma defocusing, filamentation, third harmonic generation, continuum generation, and terahertz emission [1]. Optical filamentation is usually defined as the balancing between self-focusing (Kerr effect) and plasma defocusing. The self focusing phenomenon is related to the Kerr index of refraction defined as  $n_2 I$ , with  $I$  the pulse intensity. The generally accepted value for atmospheric air,  $n_2 \approx 3 \times 10^{-19} \text{cm}^2/\text{W}$ , is deduced from self-phase modulation measurements [2]. The refractive index variation produced by the plasma is calculated from free electron density due to the ionization of air components. It has been recently proposed that the nonlinear Kerr refractive index could undergo a saturation with the intensity through a negative contribution  $n_4 I^2$ . This term was considered in order to stabilize the filament. It should be noted that no experimental value for the negative quintic parameter  $n_4$  is available. In simulations, typical values are taken within the range  $-0.25$  to  $-1 \times 10^{-32} \text{cm}^4/\text{W}^2$  [3,4]. Different work suggests that it could originate from four-wave mixing and cross-phase modulation between the fundamental and its third harmonic.

The aim of the present work is the measurement of the nonlinear refractive index of the main air components ( $\text{N}_2$ ,  $\text{O}_2$  and Ar) at filamentation laser intensities. The optical technique used for that purpose is insensitive to the plasma [5] and allows quantitative measurement from the analysis of the time-dependent laser-induced birefringence. We show that the nonlinear Kerr index exhibits a large variation and becomes negative above few tens of  $\text{TW}/\text{cm}^2$ . Drastic effects on pulse propagation are awaited from this strong nonlinear behaviour.

## 2. Polarization technique : principle and alignment contribution

The method exploits the occurrence of the post pulse molecular alignment. It is now well established that the interaction of molecules with strong ultra-short laser pulse induces periodic transient molecular alignment under field-free condition (i.e. after the pulse extinction) [6]. At the occurrence of post-pulse alignment, the sample becomes significantly birefringent. Additionally, the instantaneous Kerr effect during the pulse contributes to an extra birefringence. The principle of the technique is to compare the birefringence contribution resulting from both effects. The well known alignment signal is thus used to calibrate the instantaneous Kerr effect. The experimental setup makes use of the strong field polarization technique [7] implemented for measuring the degree of post-pulse molecular alignment. This pump-probe technique consists in measuring the birefringence of a gas sample that interacts with a "pump" pulse through the depolarization of a time-delayed weak "probe" pulse.

In the present experiment, both pulses are derived from a Ti:Sapphire chirped pulse amplified system working at 1 KHz (pulse duration of 90 fs at 800 nm). The two laser beams are focused with the same lens of focal length  $f=20$  cm and overlapped at a small angle ( $4^\circ$ ) in a gas cell. The energy of the vertically polarized pump pulse is controlled by means of a half-wave plate and a polarizer. The probe pulse is initially polarized at  $45^\circ$  with respect to the pump. The amount of depolarized light passing through a crossed analyzer, placed after the cell, is measured with a photomultiplier. The pump-probe delay is scanned by means of a motorized delay line. The expression of the homodyne signal  $S_{\text{homo}}(t)$  can be written as [8]

$$S_{\text{homo}}(t) \propto I_{\text{pr}}(t) \otimes (\Delta n(t))^2 = I_{\text{pr}}(t) \otimes (n_{\parallel}(t) - n_{\perp}(t))^2 \quad (1)$$

where  $\Delta n(t)$  is the difference of refractive index along the polarization axis  $n_{\parallel}(t)$  and perpendicular to it  $n_{\perp}(t)$ , and  $I_{\text{pr}}(t)$  is the intensity envelop of the probe pulse. Due to the quadratic response of the homodyne detection, the sign of the birefringence is lost, whereas the sensitivity is enhanced. In order to provide the sign of  $\Delta n(t)$ , heterodyne detection can be implemented by inducing an additional birefringence  $\mathcal{P}$  by means of a phase plate inserted between the two crossed polarizers. The pure heterodyne signal  $S_{\text{hetero}}(t)$  is then obtained by the subtraction of two experimental signals recorded with opposite signs of  $\mathcal{P}$  [7, 8].

$$S_{\pm}(t) \propto I_{\text{pr}}(t) \otimes (\Delta n(t) \pm \mathcal{P})^2 \quad (2)$$

$$S_{\text{hetero}}(t) = S_{+}(t) - S_{-}(t) \propto I_{\text{pr}}(t) \otimes (\mathcal{P} \Delta n(t)) \quad (3)$$

For linear molecules, the degree of alignment can be characterized by the expectation value  $\langle \cos^2 \theta \rangle$ , with  $\theta$  the angle between the molecular axis and the field [6]. The temporal dependence of alignment can be accurately calculated for linear molecules. The birefringence induced by the alignment is given by

$$\Delta n_{\text{rot}}(t) = \frac{3\rho}{4n_0\epsilon_0} \Delta\alpha \left\{ \langle \cos^2 \theta \rangle(t) - \frac{1}{3} \right\}, \quad (4)$$

with  $\Delta\alpha$  the polarizability anisotropy ( $\Delta\alpha(\text{N}_2) = 4.6$  a.u. [9],  $\Delta\alpha(\text{O}_2) = 7.25$  a.u. [10]),  $\rho$  the gas density,  $n_0$  the linear refractive index of the gas, and  $\epsilon_0$  the dielectric constant of the vacuum. The alignment signal obtained by the polarisation technique in homodyne (resp. heterodyn) detection is calculated by substituting  $\Delta n$  by  $\Delta n_{\text{rot}}$  in Eq. (1) (resp. Eq. (3)). Knowing the degree of alignment, it is thus possible to calibrate the magnitude of the other birefringence signal contributions.

### 3. Electronic Kerr terms

#### 3.1. Low field: Measurement of the nonlinear index $n_2$

The instantaneous Kerr effect produces a variation of the refractive index along the pump polarization axis defined by  $n_{\text{kerr}\parallel} = n_2 I$ . Far from any resonances, using the tensor properties of the susceptibility  $\chi^{(3)}$ , the perpendicular component can be written  $n_{\text{kerr}\perp} = \frac{1}{3} n_2 I$  [11]. The resulting birefringence is the subtraction of the refractive index between the parallel and the perpendicular axis  $\Delta n_{\text{kerr}} = \frac{2}{3} n_2 I$ . The total birefringence created by the pump beam is the sum of the rotational and the instantaneous Kerr contribution. The low field homodyne detection signal  $S_{\text{homo}}(t)$  can be then written as

$$S_{\text{homo}}(t) \propto I_{\text{pr}}(t) \otimes \left( \frac{3\rho\Delta\alpha}{4n_0\epsilon_0} \left( \langle \cos^2 \theta \rangle - \frac{1}{3} \right) + \frac{2}{3} n_2 I \right)^2. \quad (5)$$

At low intensity, the term  $n_2 I$  is sufficient to describe the Kerr effect. An experimental result obtained with nitrogen in these conditions is shown in Fig. 1. The first birefringence peak centered around the zero delay [Fig. 1(a)] is composed from the electronic ultrafast response and the inertial rotational response which is slightly delayed towards positive times (around 120 fs). The corresponding variation of the refractive index is indicated on Fig. 1(b). The full signal is fitted with expression (5) using a magnitude factor and  $n_2$  as free parameters. The post-pulse molecular alignment determines the global magnitude factor while the value of  $n_2$  is determined through the shape and the relative amplitude of the first peak. For the experiment

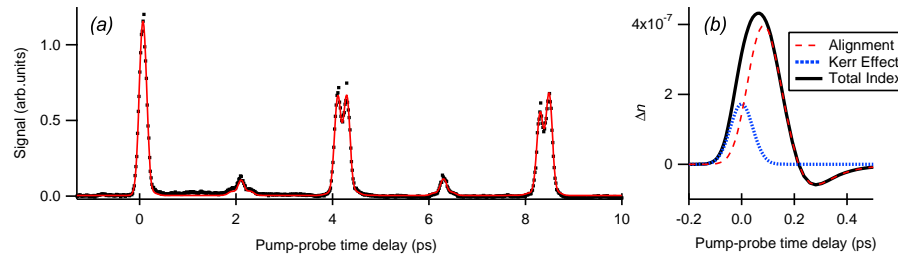


Fig. 1. (a) Recorded homodyne birefringence signal [dots] versus pump-probe delay in 1 bar of  $N_2$  at room temperature. The mean intensity of the pump is estimated around  $500 \text{ GW/cm}^2$ . The simulated signal [full line] has been adjusted to the experimental data [dots]. From this adjustment, the corresponding variation of the refractive index  $\Delta n$  (b) due to the total nonlinear birefringence [full line] composed by the instantaneous Kerr [dots] and rotational [dash] components is deduced.

performed in argon, the signal only depends on the electronic Kerr effect. It has been compared to the  $N_2$  post-pulse signal recorded separately but in the same experimental conditions as in [12]. The electronic Kerr contribution was then calibrated through the alignment of nitrogen. Compared to molecules, the uncertainty is slightly reduced, because the instantaneous and the rotational contributions are very well separated in two different signals. A statistic number of this experiment has been realized in order to considerate the additional uncertainty due to the gas change. The measured values are presented in the table 1.

Table 1. Measured  $n_2$  coefficients at 1 bar for nitrogen, oxygen, argon, and air in unit of  $10^{-7} \text{ cm}^2/\text{TW}$ .

Gas	$N_2$	$O_2$	Ar	Air
$n_2$ (Ref [2])	$2.3 \pm 0.4$	$5.1 \pm 0.7$	$1.4 \pm 0.2$	$2.9 \pm 0.4$
$n_2$ (This work)	$2.2 \pm 0.4$	$3.2 \pm 0.7$	$2.0 \pm 0.2$	$2.4 \pm 0.5$

To validate the coefficients of Table 1, the simulation of the overall signal has been successfully compared to a set of data recorded in 1 bar of air. Our values are consistent with the ones measured by Nibbering *et al.* [2] for  $N_2$ , but differ for  $O_2$  and Ar. However, they are limited to a narrower interval, as in ref. [13] although with lower predicted values (*i.e.*  $1.5 - 1.7 \cdot 10^{-7} \text{ cm}^2/\text{TW}$ ).

### 3.2. Strong field: Measurement of the higher nonlinear terms

At stronger field, the expansion of the electronic part is not sufficient to describe the whole intensity dependency of the refractive index. Pure heterodyne detection is employed here in order to obtain the sign of the birefringence  $\Delta n(t)$ . The intensity dependence for argon and nitrogen is shown in Fig. 2. To prevent any spatio-temporal distortion of the pump pulse during its propagation in the gas cell, the pressure was reduced to 100 mbar. In Fig. 2(a<sub>1</sub>) the superposition of the orientational and electronic responses results in a global positive signal around the zero delay. In contrast, at higher intensity, the signal drops rapidly and becomes negative, as evidenced by the comparison between Fig. 2(a<sub>2</sub>) and (a<sub>3</sub>) that only differ by  $\approx 20\%$  in intensity. The baseline observed for positive delay in Fig. 2(a) is due to permanent molecular alignment [6, 7] which depends on the intensity. It should be noted that simulation performed with the appropriate intensity reproduces satisfactorily the post-pulse contribution indicating a minor influence of propagation effects under the present experimental conditions.

An expansion of the Kerr development is required to justify the experimental observation around the zero delay. The refractive index variation along the polarisation axis is developed

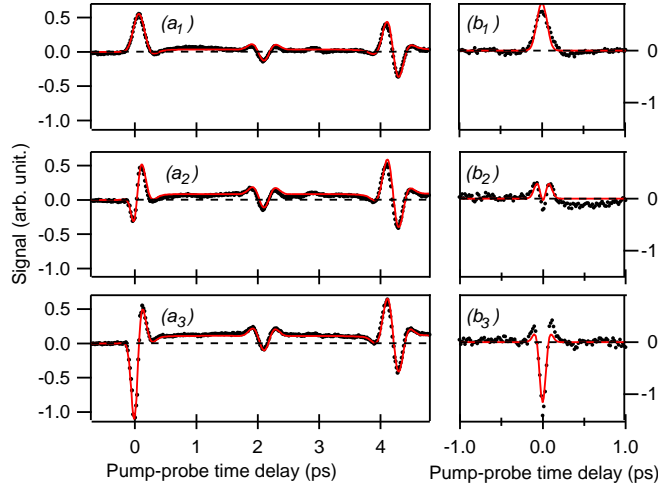


Fig. 2. Pure heterodyne signal in a 100 mbar of N<sub>2</sub> and argon at room temperature for low, medium, and high intensity. (*a*<sub>1</sub>-*a*<sub>3</sub>) N<sub>2</sub> at 22 TW/cm<sup>2</sup>, 42 TW/cm<sup>2</sup>, and 49 TW/cm<sup>2</sup>, respectively. (*b*<sub>1</sub>-*b*<sub>3</sub>) Ar at 18 TW/cm<sup>2</sup>, 24 TW/cm<sup>2</sup>, and 30 TW/cm<sup>2</sup>, respectively. A sign reversal of the Kerr component at zero delay is observed.

as  $n_{\text{kerr}} = n_2 I + n_4 I^2 + \dots + n_{10} I^5$ . In order to interpret the measurements, the birefringence resulting from each term in the series is considered. The relationship between parallel and perpendicular is known for  $n_2$  and  $n_4$  [11, 14] from the symmetry properties of the tensor  $\chi^{(3)}$  and  $\chi^{(5)}$ . This can be generalized to the higher order terms  $\Delta n_{(2 \times j)} = 2j / (2j + 1) n_{(2 \times j)} I^j$  with  $j \in \mathbb{N}^*$ . For high intensity, the pure heterodyne signal  $S_{\text{hetero}}$  becomes

$$S_{\text{hetero}}(t) \propto I_{\text{pr}}(t) \otimes \left( \underbrace{\frac{3\rho\Delta\alpha}{4n_0\epsilon_0} \left( \langle \cos^2 \theta \rangle - \frac{1}{3} \right)}_{\Delta n_{\text{rot}}(t)} + \underbrace{\frac{2}{3}n_2 I + \frac{4}{5}n_4 I^2 + \frac{6}{7}n_6 I^3 + \frac{8}{9}n_8 I^4 + \frac{10}{11}n_{10} I^5}_{\Delta n_{\text{kerr}}(t)} \right). \quad (6)$$

The determination of the higher nonlinear Kerr terms is performed as follow. We first consider the index  $n_2$  as a fixed parameter in Eq. (6) with the values given in Table. 1. The development of the instantaneous contribution is truncated at the term  $n_4$  which is thus adjusted to describe the signal in an intermediate field regime, i.e. below the intensity leading to a negative signal at zero delay. The subsequent parameters  $n_6$ ,  $n_8$ , and  $n_{10}$  are then estimated at higher intensities. The fitting procedure is similar to the one described in the previous section, namely a set of experimental records is adjusted by Eq. (6) using  $n_{(2 \times j)}$  and a magnitude factor as free parameters through a least square fitting procedure. The results are presented in Table 2. They have been corrected for the volume effect due to the spatial dependency of the laser beam. These coefficients have been confirmed by an experiment performed in 100 mbar of air. The corresponding Kerr refractive index versus intensity is displayed on Fig. 3. For all species, we see that the nonlinear refractive index linearly increases, saturates, and then drops dramatically with the intensity. It becomes negative somewhere between 19 and 33 TW/cm<sup>2</sup>, depending on the considered gas. To our best knowledge, this is the first experimental observation of a Kerr sign inversion at high intensity. We emphasize that our experimental method is not sensitive to the negative refractive index resulting from the free electrons produced by ionization, since they do not produce any birefringence. The nonlinear refractive index measured here is only due to the

Table 2. Measured coefficients of the nonlinear refractive index expansion of nitrogen, oxygen, argon, and air with  $I_{\text{inv}}$  the intensity leading to  $n_{\text{Kerr}||} = 0$ . The uncertainty corresponds to two standard deviations of the fitted values over a set of experimental records.

Gas	N <sub>2</sub>	O <sub>2</sub>	Ar	Air
$n_2$ ( $10^{-7}\text{cm}^2/\text{TW}$ )	$2.2 \pm 0.4$	$3.2 \pm 0.7$	$2.01 \pm 0.19$	$2.4 \pm 0.6$
$n_4$ ( $10^{-8}\text{cm}^4/\text{TW}^2$ )	$-0.16 \pm 0.08$	$-1.55 \pm 0.16$	$-0.11 \pm 0.31$	$-0.45 \pm 0.9$
$n_6$ ( $10^{-9}\text{cm}^6/\text{TW}^3$ )	$0.56 \pm 0.06$	$1.9 \pm 0.2$	$1.6 \pm 0.2$	$0.84 \pm 0.09$
$n_8$ ( $10^{-11}\text{cm}^8/\text{TW}^4$ )	$-2.2 \pm 0.2$	$-10.5 \pm 0.7$	$-8.6 \pm 0.5$	$-4.0 \pm 0.3$
$n_{10}$ ( $10^{-13}\text{cm}^{10}/\text{TW}^5$ )	-	-	$5.3 \pm 0.3$	-
$I_{\text{inv}}$ ( $\text{TW}/\text{cm}^2$ )	33	19	26	26

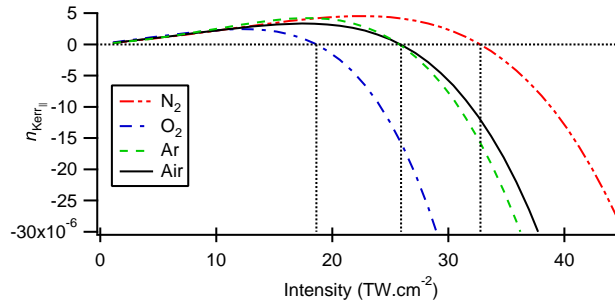


Fig. 3. Nonlinear refractive index variation of air constituents versus intensity at room temperature and 1 atm. (a) N<sub>2</sub>, (b) O<sub>2</sub>, (c) Ar, and (d) air.

bound excited electrons. The high-order terms of the Kerr effect have to be taken into account when modelling the light propagation in air. We recall that the filamentation process in gas is usually defined by the balancing between Kerr focusing and ionization defocusing. The present work suggests that the Kerr effect contributes to the defocusing mechanism. For some gases, the filamentation can be governed by the instantaneous effect, while the ionization plays a minor role [15, 16]. In general, it will strongly depends on the gas and experimental conditions.

#### 4. Conclusion

New experimental determination of the nonlinear Kerr index of refraction of N<sub>2</sub>, O<sub>2</sub>, and Ar constituents have been performed. The time resolved birefringence method allows to measure the Kerr coefficients calibrated with the postpulse molecular alignment without the detrimental plasma contribution. At high intensity, the saturation of the electronic Kerr effect is observed, followed by a sign inversion above an intensity of few tens of TW/cm<sup>2</sup> for the three gaseous components. This work reports, to our knowledge, the first experimental evidence of the sign inversion of Kerr terms at high intensity. The present result is expected to play a dominant role in the self guiding of ultrashort laser pulses. In particular, the usual description of a filament with the plasma as main defocusing contribution becomes questionable in consideration of the high-order Kerr terms revealed in the present work. An illustration of their influence reported in [15] demonstrates the possibility of plasma-free filamentation.

#### Acknowledgments

This work was supported by the Conseil Régional de Bourgogne, the ANR COMOC, and the FASTQUAST ITN Program of the 7<sup>th</sup> FP.